A Journal of the Gesellschaft Deutscher Chemiker

Angewandte International Edition Chemie

GDCh

www.angewandte.org

Accepted Article

Title: The Surface of Ice is Like Supercooled Liquid Water

Authors: Wilbert J. Smit and Huib J. Bakker

To be cited as: *Angew. Chem. Int. Ed.* 10.1002/anie.201707530
Angew. Chem. 10.1002/ange.201707530

Link to VoR: http://dx.doi.org/10.1002/anie.201707530
http://dx.doi.org/10.1002/ange.201707530

WILEY-VCH

10.1002/anie.201707530

WILEY-VCH

The Surface of Ice is Like Supercooled Liquid Water

Wilbert J. Smit and Huib J. Bakker*

Abstract: The surface of ice has been reported to be disordered at temperatures well below the bulk melting point. However, the precise nature of this disorder has been a topic of intense debate. Here, we study the molecular properties of the surface of ice as a function of temperatures using heterodyne-detected sum-frequency generation spectroscopy. We observe that, down to 245 K, the spectral response of the surface of ice contains a component that is indistinguishable from supercooled liquid water.

It is well-established that the surface of ice is disordered at temperatures well below the bulk melting point. This disordered surface governs processes as diverse as glacier motion, frost heave and chemical processes at the surface of ice particles in the atmosphere. In spite of its importance, the precise nature of the surface of ice is still under debate. For decades, the surface properties of ice have been the subject of numerous studies employing a large variety of experimental techniques.[1, 2] Much of this previous work has reached seemingly contradictory conclusions about the precise nature of the disorder of the surface of ice and its onset temperature. For example, the top surface has both been reported to resemble bulk liquid water[3, 4, 5] as well as to have a much higher viscosity than liquid water[6, 7, 8, 9, 10, 11, 12]. Recently it was also proposed that, close to the melting point, the surface of ice is made up of two phases exhibiting different morphologies (thin layers and droplets).[13, 14] The reported onset temperature for the surface disorder varies between 200 K and 271 K.[3, 15, 16, 17, 18, 19, 12]

Surface sum-frequency generation (SFG) spectroscopy is a very suitable tool to provide information on molecular surfaces as it combines surface-selectivity with molecular sensitivity. SFG relies on the enhancement of frequency mixing of visible and infrared laser pulses when the infrared pulse is resonant with vibrations of molecules at the surface. Since SFG is a second-order non-linear optical process, it is bulk-forbidden for water and ice under the electric dipole approximation.[20, 21] In this manuscript, we use SFG to study the hydrogen-bonding strength and structure of the ice surface, employing the fact that the vibrational frequencies of the OH stretch modes are strongly dependent on the strength of the hydrogen-bond interactions.[22, 23] The properties of the ice surface have been studied before with conventional intensity SFG spectroscopy. It was found that the free OH groups sticking out the ice—air interface show orientation disorder at temperatures ≥200 K, pointing at a disordered character of the top surface of ice. [10, 24] In a recent intensity SFG study on the surface of ice, a stepwise increase of the first moment of the OH stretch vibrational spectrum of the ice surface was observed, when increasing the temperature towards the melting point, indicating a rather sudden increase of the thickness of the disordered surface.[25]

The previously reported intensity spectra of ice ($I_{SFG} \sim |\chi^{(2)}|^2$, with $\chi^{(2)}$ the second-order non-linear susceptibility) represented the square of the sum of the different vibrational resonances of the ice surface and a non-resonant background[10, 24, 25]. As a result of the cross terms between the different contributions, these studies did not allow for an unambiguous identification of the spectral response of the disordered ice surface. Here, we use heterodyne-detected SFG which allows for a direct determination of the amplitude and the phase of the generated SFG electric field. The SFG field, in turn, can be directly related to the real and imaginary parts of $\chi^{(2)}$. The imaginary part of $\chi^{(2)}$ is of particular interest, as it allows a direct identification of the surface vibrational resonances. Moreover, heterodyne-detected SFG allows the separation between the resonant part of the signal and the non-resonant background, which simplifies the interpretation.[26] Using heterodyne-detected SFG, we determine the spectral response of the ice surface, and we find that this response contains a component with a spectrum that is indistinguishable from that of supercooled liquid water.

In Figure 1 we present the heterodyne-detected SFG response of the basal surface of ice at different temperatures in the range 245—270 K for an *ssp*-polarization configuration ('*ssp*' indicates that the SFG and the visible beams are *s*-polarized, i.e. perpendicular to the plane of incidence, and that the infrared beam is *p*-polarized, i.e. parallel to the plane of incidence). The imaginary part of $\chi^{(2)}$ is a sum of contributions from the different surface vibrational resonances. The inferred $|\chi^{(2)}|^2$ spectra permit a direct comparison with conventional intensity SFG measurements and are in good agreement with Refs. [24, 25]. At 245 K, the Im $\chi^{(2)}$ spectrum is dominated by an intense band at 3230 cm^{-1} with a shoulder around 3400 cm^{-1}. With increasing

[*] Dr. Wilbert J. Smit, Prof. Dr. Huib J. Bakker
AMOLF
Science Park 104, 1098 XG Amsterdam (The Netherlands)
E-mail: bakker@amolf.nl
Dr. Wilbert J. Smit
PSL Research University
ESPCI Paris
UMR CBI 8231
10 rue Vauquelin, 75005 Paris (France)

Supporting information for this article is given via a link at the end of the document

temperature the 3230 cm^{-1} band decreases in amplitude, while the shoulder around 3400 cm^{-1} increases in amplitude. The Im $\chi^{(2)}$ spectrum also shows a broad shoulder near 3550 cm^{-1}. The low amplitude of this band makes it hardly visible in the constructed $|\chi^{(2)}|^2$ spectra. We recently reported that this band can be assigned to the antisymmetric OH stretch vibration of fully coordinated interfacial water molecules and the symmetric OH stretch vibration of water molecules with two donor and one acceptor hydrogen-bond.[27] The resonance at ~3700 cm^{-1} is assigned to free OH groups sticking out from the surface. The positive sign of the imaginary part reflects their outward orientation relative to the bulk.

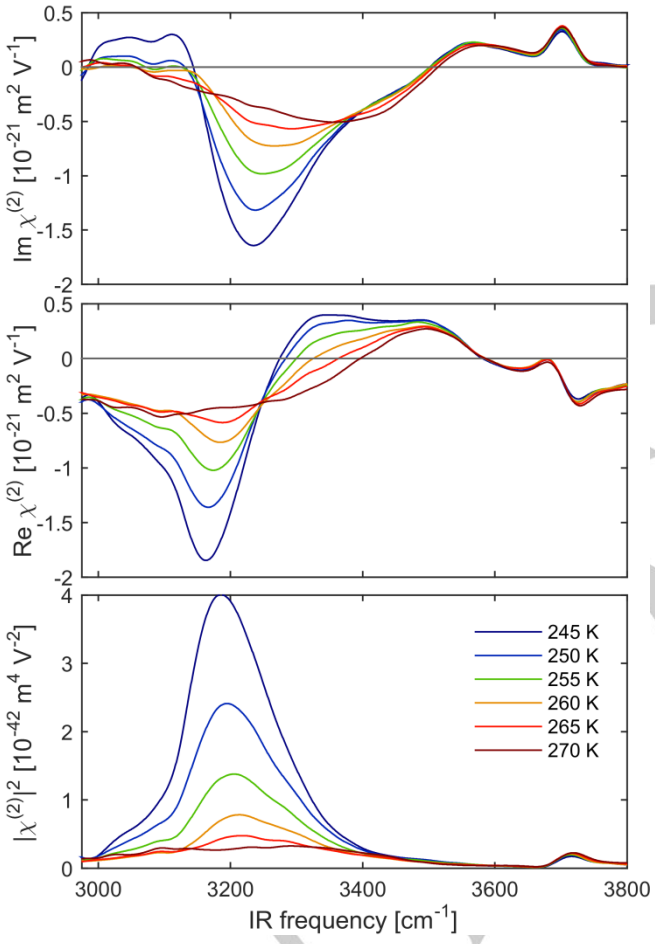

Figure 1. Second-order susceptibility of the basal surface of ice as a function of temperature. The top panel shows the imaginary component (Im $\chi^{(2)}$), the central panel the real component (Re $\chi^{(2)}$), and the bottom panel the squared amplitude ($|\chi^{(2)}|^2$).

Figure 2a displays the Im $\chi^{(2)}$ spectra of ice at 245 K, ice at 270 K, and supercooled liquid water at 270 K. In a previous study of the free OH stretch mode sticking out of the surfaces of water and ice a similar decrease in response of ice compared to water has been observed.[9] The surface Im $\chi^{(2)}$ spectrum of ice at 270 K is remarkably similar to that of supercooled liquid water at 270 K, and quite different from the surface spectrum of ice at 245 K. This indicates that the surface spectrum of ice at 270 K contains a strong contribution of a component with a similar spectral response as supercooled liquid water.

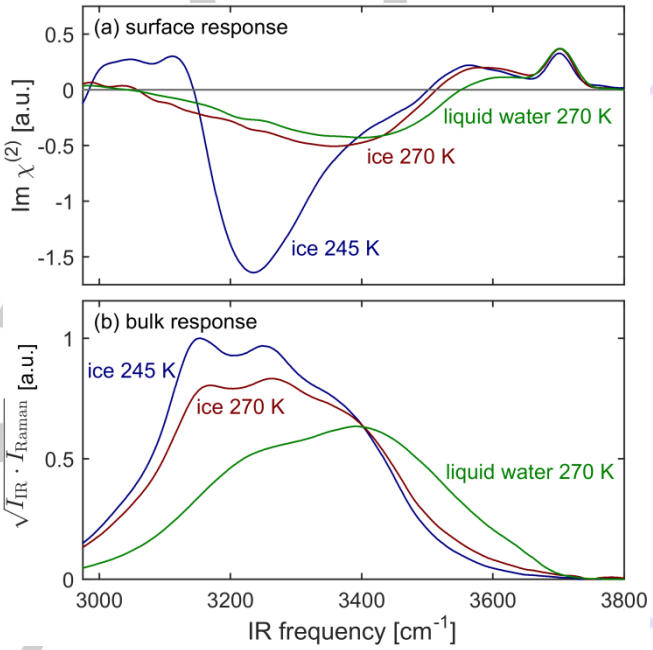

Figure 2. (a) Comparison of the imaginary parts of the surface responses (Im $\chi^{(2)}$) of the basal face of ice and supercooled water. The signals are normalized on the free OH amplitude.[10] (b) Comparison of the equivalent bulk responses (square-root-product of the infrared and Raman spectra) of ice and supercooled water. After square-root multiplication, the spectrum at 245 K is normalized to its maximum and the other two spectra are multiplied with the same normalization factor.

The bottom panel of Figure 2b shows bulk response spectra of the same systems of which the Im $\chi^{(2)}$ spectra are shown in Figure 2a. The Im $\chi^{(2)}$ spectrum of the surface can best be compared with the square root of the product of the infrared and the Raman spectrum of the bulk, as this latter constructed spectrum shows the same dependence on the infrared transition dipole moment and the Raman polarizability as $\chi^{(2)}$. The constructed spectrum of bulk ice at 270 K is quite similar to the spectrum of bulk ice at 245 K and very different from the spectrum of supercooled water at 270 K. Clearly, the bulk response of ice at 270 K is ice-like (similar to that of ice at lower

temperatures), whereas the surface response of ice at 270 K closely resembles that of supercooled liquid water.

Given this observation, we can obtain more quantitative information on the properties of the ice surface by performing a spectral decomposition (Figure 3). Previous ATR-IR studies [4] and molecular dynamics simulations [25] indicate that up to 270 K the ice surface contains only a few water-like molecular layers. Therefore we describe the ice surface as a single interfacial region comprising molecular layers of crystalline ice character and layers that are liquid-water like. We thus fit the Im $\chi^{(2)}$ spectrum of supercooled water by 3 Gaussian bands of which 2 have asymmetric widths to account for the inhomogeneity caused by varying hydrogen-bond strengths. The broad band with its maximum at 3407 cm^{-1} corresponds to hydrogen-bonded OH modes of liquid water. For the band at 3587 cm^{-1} different assignments have been reported [26, 28, 29, 30]. The band at 3702 cm^{-1} corresponds to the free OH mode. We fit the ice spectra at different temperatures with these three bands plus another asymmetric Gaussian-shaped band to account for the response around 3230 cm^{-1}, which represents the OH modes of crystalline ice. In this fit of the ice spectra at different temperatures we keep the spectral shapes and widths of the four bands constant, in order to reduce the number of free fit parameters. This approach is justified, as we fit the spectra over a relatively small temperature interval (245—270 K). With this approach we obtain a robust fit of the spectra at all measured temperatures. The peak position of the free OH band is a free fit parameter, yielding a slight shift from 3701 cm^{-1} at 245 K to 3703 cm^{-1} at 270 K. The peak position of the broad positive shoulder near 3550 cm^{-1} is kept constant at 3555 cm^{-1} based on a global fit to the ice spectra measured at different temperatures. The peak position of the band with the response of the hydrogen-bonded OH modes of liquid water is 3407 cm^{-1} at 270 K and taken to shift by 1 cm^{-1}/K. This frequency shift follows from spectra recorded for liquid water at 270 and 295 K (Figure S1). The peak position of the crystalline ice band is also set to shift by 1 cm^{-1}/K. The results of the fit are shown in Figure 3, and are seen to match the data very well.

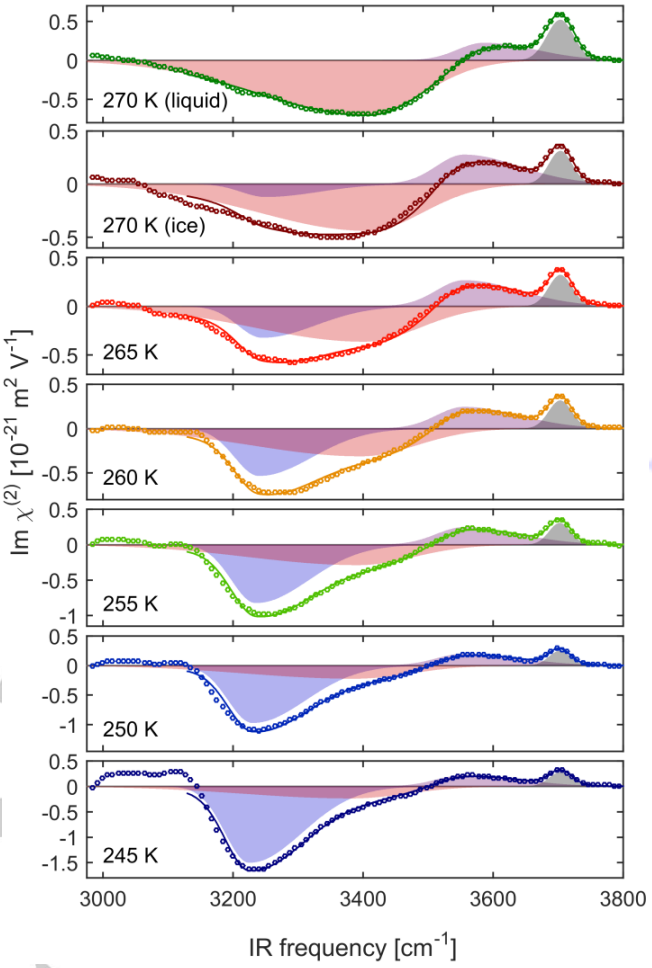

Figure 3. Spectral decomposition of the imaginary part of the susceptibility (Im $\chi^{(2)}$) of the surface of supercooled water at 270 K and the basal face of ice at temperatures between 245 and 270 K. The supercooled water spectrum (top) is fitted by a sum of two asymmetric Gaussian-shaped bands and one symmetric Gaussian-shaped band. The ice spectra are fitted with the three bands resulting from the fit to liquid water and an additional asymmetric Gaussian-shaped band (see text). The data are represented by the symbols and the fitted spectra by the solid lines. The four spectral bands that together form the fitted spectra are indicated by shaded areas. Note the different ordinate scales for the different temperatures.

The areas of the 4 bands are plotted in Figure 4 as a function of temperature. Clearly, the liquid-water like band still exhibits significant amplitude at 245 K, which is only ~2 times smaller than the amplitude of the liquid-like band measured for ice at 270 K, the surface response of ice thus shows substantial liquid-like character, even at 245 K, i.e. at 28 K below the melting point. The amplitude of the crystalline ice response strongly depends on temperature, and vanishes when approaching the melting point at 273 K (Figure 4). The amplitudes of the 3555 cm^{-1} band and the free OH band show a mild increase with temperature.

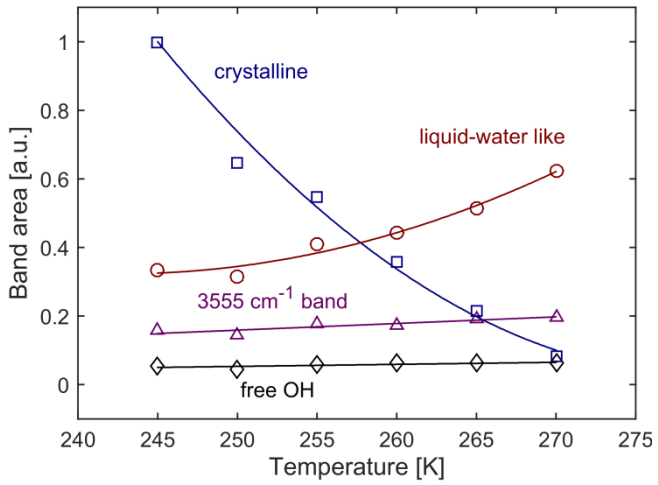

Figure 4. Areas of the crystalline ice band (~3230 cm^{-1}), the liquid-water like band (~3400 cm^{-1}), the 3555 cm^{-1} band, and the free OH band (~3700 cm^{-1}) resulting from the spectral decomposition of the ice spectra shown in Figure 2. The lines serve to guide the eye.

The observed liquid-like component probably represents the top molecular layer(s) of the ice crystal, while the measured crystalline ice response likely represents the response just underneath these top molecular layers. In previous atomic force microscopy (AFM) studies it has been reported that the viscosity of the surface layer of ice would be 300—4000 times larger than the viscosity of (supercooled) water.[9, 11, 12] In view of the present observations, it seems likely that the probed response not only represented the top molecular layers, but also included a significant contribution of the (more crystalline) layers underneath. Another explanation is that the reported high viscosities are caused by strong confinement effects between the probing tip of the atomic force microscope and the ice crystal surface.[12, 31]

In a previous spectroscopic IR-ATR study of thin ice films deposited on a germanium substrate evidence was found for the presence of two liquid-like water layers (at the ice—air and ice—germanium substrate interfaces) with a total thickness of 2 nm at 270 K, , i.e. corresponding to ~4 molecular layers (= ~2 bilayers) per interface.[4] Therefore, we tentatively attribute the observed amplitude increase of the liquid-water-like component from 0.34±0.03 at 245 K to 0.62±0.02 at 270 K to the transition from one molten bilayer of liquid-like water molecules at the surface of ice at 245 K to two molten bilayers at the surface of ice at 270 K. This explanation is supported by recent molecular dynamics simulations that reported a transition from a single disordered bilayer of water molecules at the surface of ice to two disordered bilayers, when the temperature is increased from 230 K to 270 K.[25]In summary, we determined the spectral response of the the surface of ice with heterodyne-detected surface sum-frequency generation. We find the surface to contain a component with a spectrum that is very similar to that of supercooled liquid water. This liquid-like component already shows a significant amplitude at a temperature of 245 K, i.e. at temperatures far below the melting point.

Experimental Section

The SFG experiments are performed using an amplified Ti:sapphire laser system (Coherent Legend) operating at a repetition rate of 1 kHz. This system is used to pump an optical parametric amplifier and difference-frequency mixing system delivering broadband infrared pulses with a pulse energy of 5 μJ, a central wavelength of 3.0 μm (3300 cm^{-1}) with a full width at half maximum of 0.6 μm (650 cm^{-1}), and a pulse duration of ~100 fs. The visible pulse has an energy of 15 μJ, a central wavelength of 798 nm, and a full width at half maximum of 0.9 nm (15 cm^{-1}). The bandwidth of the visible pulse determines the spectral resolution of the SFG spectra. The visible and infrared pulses are first sent in spatial overlap on a gold mirror to generate broadband sum-frequency light. This light is used as the local oscillator. Then the pulses are refocused by a concave mirror onto the sample surface with an angle of incidence of 44° for the infrared beam and 39° for the visible beam. The diameter of the beams at the sample position is ~200 μm. The SFG signal stemming from the local oscillator is delayed by a delay plate and creates an interference pattern with the SFG signal generated at the sample, which is recorded by a spectrometer equipped with a CCD camera. The signal is extracted by Fourier filtering[33] and normalized by a reference spectrum from quartz which gives a non-dispersive SFG response. The $\chi^{(2)}$ value of quartz is taken to be $8 \cdot 10^{-13}$ m V^{-1} and the coherence length is ~40 nm for our experimental configuration.[34] Next the spectra are corrected for the Fresnel factors yielding the second-order susceptibility $\chi^{(2)}$ [35, 33] using literature values for the optical constants of ice,[36] water,[37, 38] and quartz[39] and calculating the effective refractive index of the interfacial layers by the use of a slab model.[40] For an accurate determination of the phase of $\chi^{(2)}$, it is essential that the sample and reference are measured at the same height The heights of the sample and reference are set to a precision of ~1 μm, resulting in a phase inaccuracy of 10°. The obtained $\chi^{(2)}$ spectra are precisely phased such that the imaginary part is zero in the off-resonance part of the spectrum between 3800—3900 cm^{-1} conforming previous work.[41, 42, 26] During the SFG experiment, the ice sample is continuously moved to prevent the accumulation of heat and damage of the crystal (see also the Supporting Information).

Monocrystalline ice is grown by extraction of a seed from the melt.[43, 25] The orientation of the basal plane is determined by a Rigsby stage exploiting the birefringence of ice. The ice is cut to the basal plane and a flat surface is obtained by repeatedly shaving with a blade. The measurements are performed in a temperature cell that is cooled by

liquid N_2 and allows for transmittance of the laser beams through a CaF_2 window. The temperature is monitored by a thermocouple welded on the edge of the ice surface with a drop of water and the desired temperature is set by a resistance.

Linear absorption spectra are obtained with a PerkinElmer 881 double-beam IR spectrometer. Raman spectra are acquired using a Bruker SENTERRA Raman microscope by excitation by a 532 nm laser with a power of 10 mW in an unpolarized manner. The sample is prepared by pressing a water droplet between two sapphire windows for the infrared spectra and between two CaF_2 windows for the Raman spectra. The sample is placed in a cryostat allowing a precise control of the temperature (within 1 K).

Acknowledgements

This work is part of the research programme of the Netherlands Organisation for Scientific Research (NWO) and was performed at the research institute AMOLF. We thank Mischa Bonn and Ellen Backus for helpful discussions. We would also like to thank Hinco Schoenmaker and Dion Ursem for technical support, and Walter Scholdei for measuring the Raman spectra.

Keywords: ice • surface melting • sum-frequency generation • vibrational spectroscopy • IR spectroscopy

[1] J. G. Dash, A. W. Rempel, J. S. Wettlaufer, *Rev. Mod. Phys.* **2006**, *78*(3), 695–741.

[2] T. Bartels-Rausch, H.-W. Jacobi, T. F. Kahan, J. L. Thomas, E. S. Thomson, J. P. D. Abbatt, M. Ammann, J. R. Blackford, H. Bluhm, C. Boxe, F. Domine, M. M. Frey, I. Gladich, M. I. Guzmán, D. Heger, T. Huthwelker, P. Klán, W. F. Kuhs, M. H. Kuo, S. Maus, S. G. Moussa, V. F. Mcneill, J. T. Newberg, J. B. C. Pettersson, M. Roeselová, J. R. Sodeau, *Atmos. Chem. Phys.* **2014**, *14*(3), 1587–1633.

[3] Y. Furukawa, M. Yamamoto, T. Kuroda, *J. Cryst. Growth* **1987**, *82*(4), 665–677.

[4] V. Sadtchenko, G. E. Ewing, *J. Chem. Phys.* **2002**, *116*, 4686; V. Sadtchenko, G. E. Ewing, *Can. J. Phys.* **2003**, *81*(1–2), 333–341.

[5] B. F. Henson, L. F. Voss, K. R. Wilson, J. M. Robinson, *J. Chem. Phys.* **2005**, *123*(14), 144707.

[6] H. H. G. Jellinek, *J. Colloid Interface Sci.* **1967**, *25*(2), 192 – 205.

[7] S. Barer, N. Churaev, B. Derjaguin, O. A. Kiseleva, V. D. Sobolev, *J. Colloid Interface Sci.* **1980**, *74*(1), 173–180.

[8] N. V. Churaev, S. A. Bardasov, V. D. Sobolev, *Colloids Surf., A* **1993**, *79*(1), 11–24.

[9] H. J. Butt, A. Döppenschmidt, G. Hüttl, E. Müller, O. I. Vinogradova, *J. Chem. Phys.* **2000**, *113*(3), 1194–1203.

[10] X. Wei, P. B. Miranda, Y. R. Shen, *Phys. Rev. Lett.* **2001**, *86*(8), 1554–1557.

[11] B. Pittenger, S. C. Fain, M. J. Cochran, J. M. K. Donev, B. E. Robertson, A. Szuchmacher, R. M. Overney, *Phys. Rev. B* **2001**, *63*, 134102.

[12] M. P. Goertz, X.-Y. Zhu, J. E. Houston, *Langmuir* **2009**, *25*(12), 6905–6908.

[13] G. Sazaki, S. Zepeda, S. Nakatsubo, M. Yokomine, Y. Furukawa, *Proc. Natl. Acad. Sci. USA* **2012**, *109*(4), 1052–1055.

[14] H. Asakawa, G. Sazaki, K. Nagashima, S. Nakatsubo, Y. Furukawa, *Proc. Natl. Acad. Sci. USA* **2016**, *113*(7), 1749–1753.

[15] M. Elbaum, S. G. Lipson, J. G. Dash, *J. Cryst. Growth* **1993**, *129*(3), 491–505.

[16] A. Lied, H. Dosch, J. H. Bilgram, *Phys. Rev. Lett.* **1994**, *72*(22), 3554–3557.

[17] H. Dosch, A. Lied, J. Bilgram, *Surf. Sci.* **1995**, *327*(1–2), 145–164.

[18] A. Döppenschmidt, H.-J. Butt, *Langmuir* **2000**, *16*(16), 6709–6714.

[19] H. Bluhm, D. F. Ogletree, C. S. Fadley, Z. Hussain, M. Salmeron, *J. Phys.: Condens. Matter* **2002**, *14*(8), L227.

[20] H. Groenzin, I. Li, M. J. Shultz, *J. Chem. Phys.* **2008**, *128*(21), 214510.

[21] Y. R. Shen, *Annu. Rev. Phys. Chem.* **2013**, *64*(1), 129–150.

[22] C. J. Fecko, J. D. Eaves, J. J. Loparo, A. Tokmakoff, P. L. Geissler, *Science* **2003**, *301*(5640), 1698–1702.

[23] H. J. Bakker, J. L. Skinner, *Chem. Rev.* **2010**, *110*(3), 1498–1517.

[24] X. Wei, P. B. Miranda, C. Zhang, Y. R. Shen, *Phys. Rev. B* **2002**, *66*(8), 085401.

[25] M. A. Sánchez, T. Kling, T. Ishiyama, M.-J. van Zadel, P. J. Bisson, M. Mezger, M. N. Jochum, J. D. Cyran, W. J. Smit, H. J. Bakker, M. J. Shultz, A. Morita, D. Donadio, Y. Nagata, M. Bonn, E. H. G. Backus, *Proc. Natl. Acad. Sci. USA* **2017**, *114*(2), 227–232.

[26] I. V. Stiopkin, C. Weeraman, P. A. Pieniazek, F. Y. Shalhout, J. L. Skinner, A. V. Benderskii, *Nature* **2011**, *474*(7350), 192–195.

[27] W. J. Smit, F. Tang, Y. Nagata, M. A. Sánchez, T. Hasegawa, E. H. G. Backus, M. Bonn, H. J. Bakker, *J. Phys. Chem. Lett.* **2017**, *8*, 3656–3660.

[28] Y. Nagata, T. Hasegawa, E. H. G. Backus, K. Usui, S. Yoshimune, T. Ohto, M. Bonn, *Phys. Chem. Chem. Phys.* **2015**, *17*(36), 23559–23564.

[29] J. Schaefer, E. H. G. Backus, Y. Nagata, M. Bonn, *J. Phys. Chem. Lett.* **2016**, *7*(22), 4591–4595.

[30] Y. Suzuki, Y. Nojima, S. Yamaguchi, *J. Phys. Chem. Lett.* **2017**, *8*, 1396–1401.

[31] Y. Li, G. A. Somorjai, *J. Phys. Chem. C* **2007**, *111*(27), 9631–9637.

[32] V. Sadtchenko, G. E. Ewing, *Can. J. Phys.* **2003**, *81*(1–2), 333–341.

[33] S. Nihonyanagi, S. Yamaguchi, T. Tahara, *J. Chem. Phys.* **2009**, *130*(20), 204704.

[34] X. Wei, S.-C. Hong, X. Zhuang, T. Goto, Y. R. Shen, *Phys. Rev. E* **2000**, *62*, 5160–5172.

[35] H.-F. Wang, W. Gan, R. Lu, Y. Rao, B.-H. Wu, *Int. Rev. Phys. Chem.* **2005**, *24*(2), 191–256.

[36] S. G. Warren, R. E. Brandt, *J. Geophys. Res.* **2008**, *113*, D14220.

[37] M. R. Querry, D. M. Wieliczka, D. J. Segelstein, Water (H_2O) in *Handbook of Optical Constants of Solids II* (Hrsg.: E. D. Palik), Academic Press, **1991**, S. 1059–1077.

[38] A. Y. Zasetsky, A. F. Khalizov, M. E. Earle, J. J. Sloan, *J. Phys. Chem. A* **2005**, *109*(12), 2760–2764.

[39] I. H. Malitson, *J. Opt. Soc. Am.* **1965**, *55*(10), 1205–1209.

[40] X. Zhuang, P. B. Miranda, D. Kim, Y. R. Shen, *Phys. Rev. B* **1999**, *59*(19), 12632–12640.

[41] S. Yamaguchi, *J. Chem. Phys.* **2015**, *143*(3), 034202.

[42] S. Nihonyanagi, R. Kusaka, K.-I. Inoue, A. Adhikari, S. Yamaguchi, T. Tahara, *J. Chem. Phys.* **2015**, *143*(12), 124707.

[43] D. S. Roos, *J. Glaciol.* **1975**, *14*(71), 975.

10.1002/anie.201707530

WILEY-VCH

Entry for the Table of Contents

COMMUNICATION

The molecular properties of the surface of ice are studied in the temperature region 245—270 K using heterodyne-detected sum-frequency generation spectroscopy. We observe that, down to 245 K, the spectral response of the quasi-liquid layer is indistinguishable from that of supercooled liquid water.

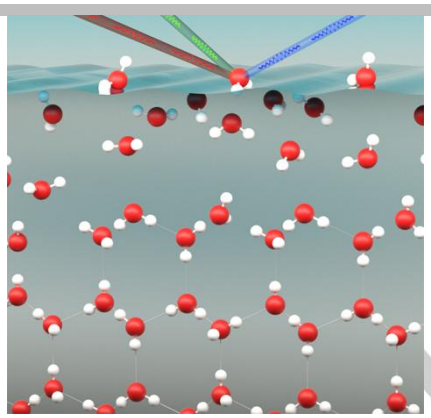

*Wilbert J. Smit, Huib J. Bakker**
Page No. – Page No.
The Surface of Ice is Like Supercooled Liquid Water

Supporting Information

The Surface of Ice is Like Supercooled Liquid Water

Wilbert J. Smit[†,‡] and Huib J. Bakker[*,†]

†*AMOLF, Science Park 104, 1098 XG Amsterdam, The Netherlands*

‡*PSL Research University, ESPCI Paris, UMR CBI 8231, 10 rue Vauquelin, 75005 Paris, France*

E-mail: bakker@amolf.nl

Spectral decomposition of liquid water–air spectra

A spectral decomposition of the Im $\chi^{(2)}$ responses of the liquid water-air interface at 270 and 295 K is given in Figure S1 .

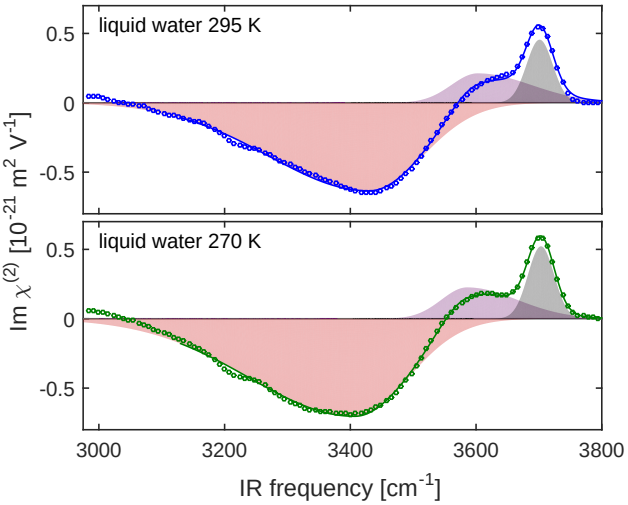

Figure S1: Spectral decomposition of the Im $\chi^{(2)}$ spectrum of the liquid water-air interface at 270 and 295 K. The spectra are decomposed in two asymmetric Gaussian bands and one symmetric Gaussian band. The maximum of the negative imaginary band is found to be located at 3407 cm^{-1} for 270 K and at 3430 cm^{-1} for 295 K, corresponding to a shift of $\sim$1 cm^{-1}/K.

Effect of laser-induced heating

Potentially there are two heating effects that could influence the measurements. The first effect is direct heating occurring during the excitation pulse, and the second is accumulated heating as a result of the repetitive excitation of the sample. The effect of direct heating on the spectrum is determined by the amount of energy dissipated by a single infrared laser pulse in the excited volume (determined by the absorption length), and the relaxation and thermalization time constants. In our experiment, the infrared pulsed reaching the ice surface have a pulse energy of $\sim$3 μJ. The bandwidth of the infrared pulse (650 cm^{-1} full width at half maximum) is broader than the bulk absorption of ice (300 cm^{-1} full width at half maximum). As a result, about 1.5 μJ infrared light is absorbed in the first micron depth of the ice surface. The infrared beam is focussed to $\sim$0.2 mm at the ice surface. Using a volumetric heat capacity of ice of $2 \cdot 10^6$ J m^{-3} K^{-1} this results in a local heat jump of $\sim$13 K, after the relaxation and thermalization of the energy of the excitation pulse is complete. The SFG signal is generated within the infrared pulse duration of 100 fs because the dephasing time is very short ($<$10 fs). The T_1 relaxation time of the excited OH vibrations of ice is $\sim$300 fs,[S1,S2] which implies that only part of the excited OH vibrations will have relaxed within the infrared pulse duration. Moreover, the vibrational relaxation does not directly lead to thermalization. For ice the vibrational relaxation is followed by a much slower thermalization process that takes place on a time scale of several picoseconds.[S1,S3] This latter slow thermalization process governs the effect of the excitation on the OH stretch spectrum. As a result, the effect of heating on the OH stretch spectrum will be very small within the 100 fs of the infrared pulse duration, corresponding to a temperature increase $<$1 K.

The second potential heating effect is accumulated heating. We avoid this effect by continuously moving the ice sample through the laser foci. To experimentally test the potential effect of direct and accumulated heating effects on the SFG spectra we varied the excitation energy and the speed of the actuators moving the sample. As can be seen in Figure S2,

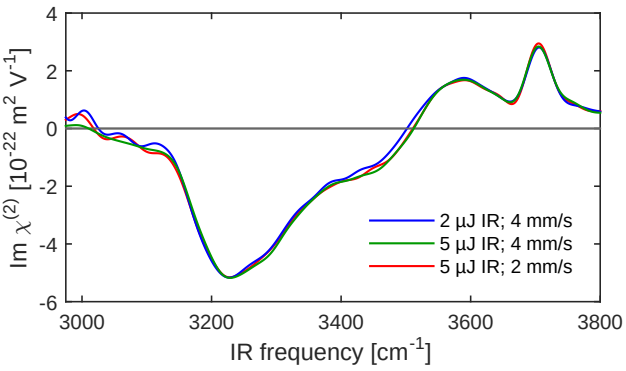

Figure S2: SFG spectra of the ice surface obtained with various infrared intensities and moving speeds of the ice sample at ∼250 K. The sample is of a different cut than the one used in the main manuscript. Both a reduction in intensity of the infrared pulses from 5 μJ to 2 μJ and a reduction in the moving speed from 4 mm/s to 2 mm/s do not affect the spectral shape.

the spectrum has similar shape and amplitude for different excitation energies and moving speed conditions. Therefore, we conclude that the heating effect of the laser pulses on the SFG spectra is very small. Hence, both direct and accumulated heating effects are found to be negligible in our experiment.

References

[S1] Timmer, R. L. A.; Bakker, H. J. *J. Phys. Chem. A* **2010**, *114*, 4148–4155.

[S2] Perakis, F.; Hamm, P. *Phys. Chem. Chem. Phys.* **2012**, *14*, 6250–6256.

[S3] Iglev, H.; Schmeisser, M.; Simeonidis, K.; Thaller, A.; Laubereau, A. *Nature* **2006**, *439*, 183–186.